

Design for an 8 m telescope with a 3 degree field at f/1.25 - the Dark Matter Telescope

Roger Angel, Michael Lesser, & Roland Sarlot

*The University of Arizona, Steward Observatory, 933 N. Cherry Ave.,
Tucson, AZ 85721*

Edward Dunham

Lowell Observatory, 1400 W. Mars Hill Rd., Flagstaff, AZ 86001

Abstract. Deep images recorded over a wide field of view are needed for astronomical projects as diverse as measuring cosmological parameters by weak gravitational lensing and predicting asteroid collisions with the Earth. Here we give the design for a three-mirror, 8.4 m telescope with an etendue of $260 (m.^{\circ})^2$, ten times greater than any other current or planned telescope. Its 3° diameter field is formed at f/1.25, and would be recorded by 55 cm diameter circular mosaics of CCDs for wavelengths $0.3 - 1\mu\text{m}$ and HgCdTe devices for $1 - 2.4\mu\text{m}$. The plate scale of $51\mu\text{m}/\text{arcsec}$ ensures that seeing-limited images will be well sampled by the 10 - $15\mu\text{m}$ pixel sizes of these detectors. When used to integrate single deep images over its 7 square degree field of view, the limiting magnitude (10σ) for a 1 night exposure will be U=26.7, B=27.8, V=27.9, R=27.6, I=26.8, J=24.8, H=23.5 and Ks=22.8. When used to find faint moving or variable objects by quickly imaging large fields, the telescope will be repositioned in 5 seconds while the detector mosaic is read out. Such agility is realized because the telescope is centrally balanced and very compact, little longer than the primary mirror diameter. By repositioning every 30 seconds, 1 steradian per night could be imaged to a limiting magnitude (10σ) of $V > 24$ or $K_s > 19$. For spectroscopic follow-up, several hundred integral field units could be used to study rare objects identified by imaging but too faint and sparsely scattered for efficient follow-up with any other large telescope.

1. Rationale and design considerations

Much of today's cutting edge astronomy makes use of just two types of optical telescope: ground based instruments having huge light grasp but with image quality limited by atmospheric blurring, and the Hubble space telescope with small aperture but exquisite image quality. In the future, larger cooled telescopes with unique sensitivity in the infrared are planned for space, while ground based telescopes will be much improved through correction of atmospheric blurring with adaptive optics. Interferometers will give still higher resolution, though at the price of proportional reduction in both field and sensitivity.

Here we consider a new type of ground based telescope, one whose strength lies not in a small, diffraction limited field of view but in having the widest possible field with the largest aperture. Equipped with a large mosaic of detectors to reach sensitivity limits set only by sky photon noise and atmospheric seeing, such a telescope has unique scientific potential. It would also be used to probe fields as large as the whole sky to unprecedented depth. By taking advantage of massive computational power only now becoming available, it would be able to identify very faint moving and variable objects. Many scientific projects are already envisaged for this Dark Matter Telescope, as described by Armandroff et al. (1999). It will also doubtless be used for projects as yet undreamed of, undertaken with the legacy of a truly enormous data base as well as with new observations.

A general measure of the power of a telescope is the figure of merit $A\Omega\eta/d\Omega$. Here A is the collecting area, Ω the solid angle of the field of view, η the detector quantum efficiency and $d\Omega$ the solid angle of the seeing limited image. In given integration time the size of field larger than Ω that can be explored to given depth is directly proportional to this figure of merit. While longer integration times can sometimes compensate for a lower figure of merit due to reduced image quality or smaller field or aperture, for some specific projects individual factors are decisive. For example, good image quality is essential to detect dark matter by slight changes in shape of distant galaxies, while long exposures cannot substitute for large aperture and good image quality in the detection of very faint moving asteroids.

To maximize the figure of merit for an imaging telescope, it should be in a site with excellent seeing and its focal length must be chosen so the detector pixels will adequately sample seeing-limited images. Experience shows that good telescopes at the best sites will deliver images of 0.5 arcsec on occasion, more frequently in the near infrared. The pixel sampling should be no worse than 0.25 arcsec (the Nyquist sampling criterion) to avoid further significant image degradation, thus each square degree on the sky must be sampled by about 200 million pixels in the detector mosaic. We would like to cover the 0.3 - 2.4 micron spectral range where the atmosphere is largely transparent and has relatively low emissivity. This will require two detector array types, most likely silicon CCDs below 1 μm wavelength and HgCdTe arrays above. Both types have quantum efficiencies, η , near unity. Individual 2048 x 2048 arrays of HgCdTe will be practical in the near future with 15 μm pixels, but not much smaller (Vural, 1999). This pixel size is consistent with future CCDs with high full well capacity, as we discuss below. Thus the optimum focal length should be around 10 - 12 m.

We have investigated optical designs for telescopes to deliver the largest possible aperture and field consistent with this focal length, with minimal degradation of 0.5 arcsec images. The largest convenient monolithic primaries are 8 m diameter, which would require imaging at f/1.25 to obtain 10 m focal length. Conventional telescope designs, including Schmidt cameras and other corrected systems based on one or two mirrors are incapable of wide fields at so fast a focus, but three-mirror optical systems have this capability, as we now show.

2. Three mirror telescope design

2.1. Paul optics

Three-mirror telescopes were first explored by Paul (1935). He gave a design with a parabolic primary, convex spherical secondary and a concave spherical tertiary of equal but opposite curvature. The image is formed midway between secondary and tertiary, with good correction over a wide field. One can think of the design as a reflective Schmidt telescope used as a corrector for a large afocal Cassegrain telescope. The secondary, located at the center of curvature of the tertiary, has added correction for spherical aberration in the manner of a reflecting Schmidt plate. A telescope of this type with a one degree field was built by McGraw et al., (1982), using a 1.8 m parabolic primary at $f/2.2$. The central obscuration was 22% by area, and the design gave images no more than 0.2 arcsec rms diameter at the edge of the field.

The Paul geometry is capable of still wider fields at fast focal ratio, when vignetting and central obscuration are minimized. We have explored general 3-mirror systems using ZEMAX, allowing all three mirrors to have aspheric figure optimized specifically for wide field. The wide field was not constrained to be flat, since the dedicated detector mosaics can be configured to approximate a curved field, with each flat device tangent to the focal surface.

Our first investigations were very encouraging in that we found that well corrected fields of 3° diameter or more can be formed at $f/1$ by the three mirrors alone. As the field is increased beyond 3° , so are the losses due to vignetting and central obscuration. Obscuration is caused by the large secondary and tertiary blocking the primary and by the detector obscuring the beam to the tertiary. Sky baffles needed to prevent any non-focused light from getting to the detector also increase obscuration and vignetting. An optimum design balances obscuration and field of view to maximize etendue or $A\Omega$ product for given primary aperture.

In a preprint circulated at the Austin AAS meeting (Angel, Dunham, Lesser and Millis, January, 1999), we gave a 3-mirror design with 3° diameter field and 25% central obscuration with little vignetting. While this design achieved the basic goals, it had significant limitations. The image formed at $f/1$ by a 6.5 m telescope had an uncomfortably small plate scale of $31 \mu\text{m}/\text{arcsec}$. The design also had poor achromaticity because of the introduction of a dewar window. Despite making this as thin as we dared (7 mm of sapphire), longitudinal chromatic aberration limited the breadth of filter passbands. Furthermore, to minimize vignetting there was inadequate room for thermal baffling around the detectors, or for filters to be stored in the dewar.

2.2. Revised design

Recognizing these difficulties, we have developed a more practical design with the tertiary mirror located significantly behind the primary (figure 1). The advantages of this placement for wide field imaging were recognized by Willstrop (1984). To minimize the secondary obscuration, the primary focal ratio was held at $f/1.0$, but we have used the added design flexibility to achieve a slower final focal ratio of $f/1.25$ for a better match to detector pixels. In a second major improvement, we have introduced a robust fused silica meniscus element to act as a vacuum window for the detector dewar (figure 2). This refractive element

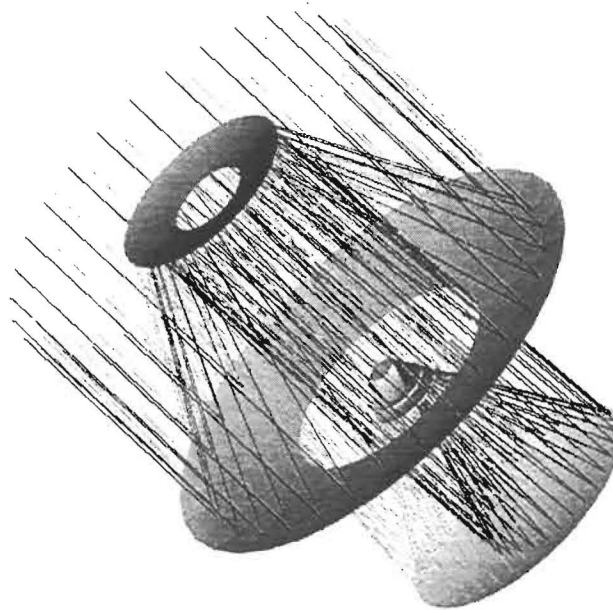


Figure 1. Optical layout with rays at $\pm 1.5^\circ$ field angle.

together with the assigned 5 mm thick passband filter would together introduce unacceptable chromatic aberration, but this is corrected by a second, negative lens of fused silica located inside the dewar. The non-chromatic aberrations of the two lenses are balanced by reoptimization of the three reflecting elements, and by allowing the concave, inside surface of the dewar window to be aspheric. In this way the effects of longitudinal and chromatic aberration are almost eliminated. We are currently investigating the possibility that the internal element could be modified to include prisms or lenses to correct also for atmospheric dispersion.

The mirrors are arranged so the light from the secondary passes through a half-diameter hole in the primary to a near-spherical tertiary behind, and is brought to a focus near the primary vertex. Detector obscuration is minimized by making the primary and secondary together afocal. With these choices, the 3° field is completely baffled against stray sky light illumination with total obscuration and vignetting held to 26% at the field center and rising to 38% at the field edge.

The optical prescription for the new design (slightly different dewar optics are used for the infrared) are given in table 1. The dimensions are for 8.4 m primary aperture, which results in a focal length of 10.5 m, and a plate scale $51 \mu\text{m}/\text{arcsec}$. The 3° field has diameter 55 cm and is nearly flat, with a radius of curvature of 10 m (sagittal depth of 2.6 mm). The specific primary diameter of 8.4 m was chosen because similarly aspheric mirrors of this size are currently in production at the University of Arizona Mirror Lab (at $f/1.14$), and advantage could be taken of existing tooling, handling fixtures and test equipment. Such a large primary is preferred both because of its large light grasp and to obtain the

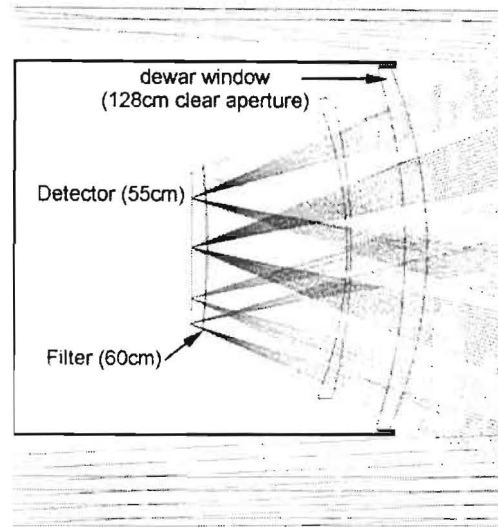


Figure 2. Detail of the dewar optics. The right hand positive meniscus lens 1.3 m in diameter forms the vacuum entrance window. The negative meniscus lens is an internal corrector. Just ahead of the focal surface is a bandpass filter.

optimum system focal length as long as 10.5 m. The telescope has an effective (unobscured) diameter of 6.9 m averaged over the field, and a collecting area of 38 m². Given detector mosaics to cover the full 3° circular field, the etendue is 260 (m.°)².

Table 1. Prescription for system configured with optical camera

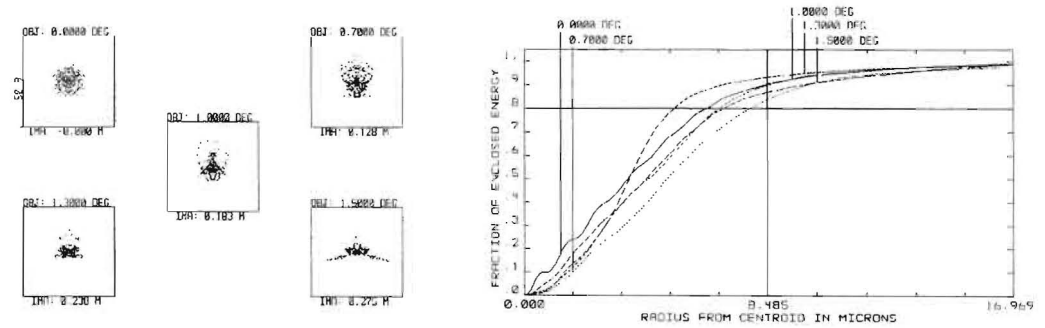
Surface	Radius	Thickness	Dia.	Conic	r ⁶	r ¹⁰	r ¹⁶
Primary	-16.80000	-5.09996	8.40	-1.027354	-7.794474e-9	-7.959556e-13	1.808951e-18
Secondary	-6.59999	3.98969	3.43	-0.597477	-1.104251e-5	-7.162328e-8	1.858206e-10
Tertiary	-8.26926	-3.29459	4.45	-0.068663	-2.460928e-8	-6.114825e-10	1.788511e-12
window	-1.71869	-0.07875	1.28	0	0	0	0
(silica)	-2.16001	-0.19262	1.28	-0.201983	0.003512024	-0.004189095	0.0214793
Corrector	-2.31283	-0.01562	1.12	0	0	0	0
(silica)	-1.49723	-0.51128	1.07	0	0	0	0
Filter	-2.89751	-0.00525	0.59	0	0	0	0
(silica)	-2.89751	-0.04114	0.58	0	0	0	0
Detector	-10.00685		0.55	-67.59419	-0.0067470		

2.3. Image quality

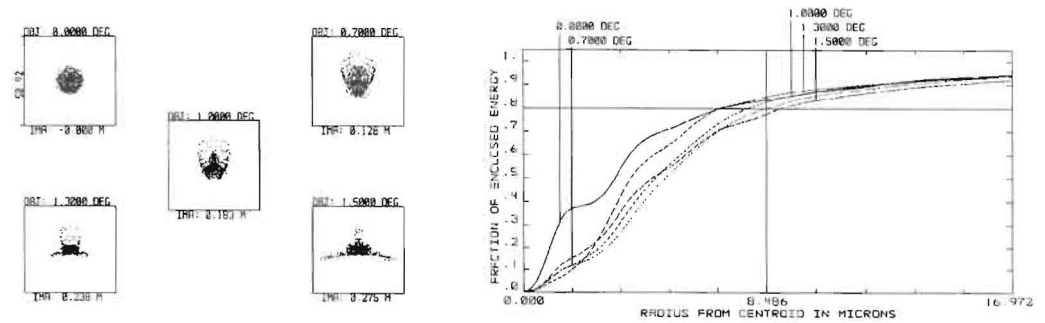
The telescope prescription was optimized for field angles 0, 0.7, 1.0, 1.3 and 1.5°, and for a single very broad band covering 0.45 - 0.75 μm. Such a broad band covering the darkest sky background is of practical value to reach the faintest asteroids, whose images would be trailed in the longer exposures needed for typical photometric bands. We obtain at least 80% energy encircled within 1/3 arcsec diameter for all field positions, despite the broad chromatic range. Such achromaticity in the presence of a thick vacuum window represents a significant advance over previous Paul designs.

For the full range of optical photometric passbands, U - z, similar quality is obtained by adjusting the mirror spacings by a few mm to refocus and compensate small wavelength-dependent aberrations. Such adjustments are within the range of mirror support systems. As an example of a typical photometric band, we show in figure 3a the images that would be recorded in the R band, by combining spot diagrams for $0.6 + 0.65 + 0.7 \mu\text{m}$. All field angles show better than 80% energy into $1/3$ arcsec.

For the infrared camera, the design of the silica window and internal corrector element in the dewar was re-optimized for wavelengths $1.25 + 1.65 + 2.2 \mu\text{m}$ taken all together. Even for this very broad band, all the images are within the target of 80% into $1/3$ arcsec diameter except at the very edge. In practice, refocus allows the target to be met in any one of the J, H or K bands observed individually. The images shown in figure 3b are for the H band.



a) 0.6, 0.65, and $0.7 \mu\text{m}$



b) 1.475, 1.65, and $1.825 \mu\text{m}$

Figure 3. Left: spot diagrams for field angles up to 1.5° off-axis. The box size is 1 arcsec. Right: encircled energy as a function of aperture radius. The marked point is for 80% energy in $1/3$ arcsec diameter.

2.4. Sky Baffling

Through most of the telescope's spectral range, up to $1.8\mu\text{m}$, its sensitivity is limited by photon noise from optical emission by the atmosphere. To prevent additional skylight from reaching the focal surface indirectly, two black conical baffles will be used. The first, 4 m in diameter, extends 0.5 m below the secondary mirror (see figure 4). The second, 3.8 m diameter, rises 1.1 m above the primary hole. These two give complete sky baffling out to the full 1.5° field angle.

Above 2 microns wavelength black body thermal emission from telescope surfaces rises rapidly and would be the dominant background in the K band. To minimize such emission it is normal to use re-imaging optics in the dewar, so as to create an entrance pupil image where a cold stop can be located. For this telescope with very large field and fast focal ratio, pupil reimaging is prohibitively difficult and a new strategy is required. As is conventional, we will remove the upper baffle, so the secondary is seen against the colder sky background. In addition, the infrared mosaic detector is set back in the dewar, 0.8 m behind a 1.3 m diameter cold baffle just inside the entrance aperture. This reduces the solid angle accepting thermal radiation through the window to 1.4 steradians, still about 3 times the solid angle of the f/1.25 beam (0.45 ster). To further reduce this external radiation we take advantage of the fact that the dewar window viewed from the outside is a large surface with extremely low emission in the K band. Thus to block radiation from the lower "tube" supporting the tertiary mirror which is viewed directly by the detector, we propose to line it with gold-coated retro-reflectors. These would be curved mirror segments with their center of curvature on the dewar window. Radiation from other telescope surfaces seen reflected in the tertiary, such as the back of the primary, will be similarly blocked by placing in front of them flat retro-reflectors. In this way, we expect that the effective emissivity over the 1.4 steradians opening could be reduced to 0.2. This would cause a thermal background equivalent to that of 60% emissivity in the f/1.25 beam. From the estimates given by Gillett and Mountain (1998), thermal emission at this level would equal the OH background at $2.2\mu\text{m}$, would be ten times stronger at $2.4\mu\text{m}$ and 4 times weaker at $2.0\mu\text{m}$. Thus the sensitivity should be little compromised in the Ks band, from 2 to $2.2\mu\text{m}$.

3. Practical aspects

3.1. Mirrors, windows and filters

The three large aspheric mirrors needed for the telescope are manufacturable by methods already proven at the Mirror Lab (Martin et al. 1998). The primary is similar to the very fast 8.4 m f/1.14 mirrors for the Large Binocular Telescope, now in process. Already the f/1.25, 6.5 m Magellan I mirror has been finished to the diffraction limit at $0.5\mu\text{m}$. The 4.5 m concave tertiary is very fast, f/0.8, but is not very aspheric, and should not present any great difficulty. Perhaps the most challenging mirror is the smallest, the convex 3.5 m secondary. A similarly aspheric 1.6 m Cassegrain secondary for the MMT (Smith et al. 1997) is being made at the Mirror Lab, with stressed lap figuring and a computer-generated,

full aperture holographic test plate. The same methods would be extended to 3.5 m turntables for the figuring and hologram manufacture.

The dewar windows are 1.3 m diameter, and must take vacuum loading at sea level of about 14 tons. Their convex meniscus shape is favorable, adding shell stiffness; a preliminary finite element study kindly made by Warren Davison finds no stresses larger than 1000 psi for the shape given in the prescription, 79 mm thick at the center and 50 mm at the edge. The window would be figured with slightly more curvature than needed, to allow for the flattening under load.

We envisage intermediate waveband filters made by multi-layer coatings deposited on meniscus glass substrates 60 cm in diameter. In any optical systems with large etendue, the sharpness of interference filters is limited by the inevitable lack of collimation. Spectral broadening is proportional to the solid angle of rays passing through the filter. The smallest possible solid angle passing through a filter of area a_f is $A\Omega/a_f$. Filters 60 cm in diameter to cover the 3° field at $f/1.25$ will produce broadening $\Delta\lambda/\lambda$ of about 3%, a practical lower limit for broadening. George Jacoby has kindly calculated the profile of a 24 nm wide filter at 555 nm ($\Delta\lambda/\lambda = 4\%$), and finds the width is little affected compared to illumination at normal incidence, but the sides become less steep.

3.2. Detectors

CCD detector arrays are now a rather mature technology, and there is little doubt that a mosaic to cover the full 55 cm circular focal surface can be built for acceptable cost. One camera equipped with such a mosaic would alone be sufficient for the key dark matter and asteroid mapping projects. A similarly sized mosaic of infrared detectors represents a greater leap, but is nevertheless feasible and has enormous potential for study of the universe at high redshift and as a precursor to NGST. In both cases the individual flat detector arrays will be arranged in the form of a slightly domed mosaic to best fit the focal surface. There will remain some defocus across each flat array, but this can be held to acceptable level. Thus the 10 m radius of curvature of the focal plane results in only $\pm 8\mu\text{m}$ of longitudinal defocus for individual square arrays 25 mm on a side.

CCD mosaic A significant issue for CCDs is the control of charge blooming from bright stars. Deep wells, anti-blooming measures and the use of many smaller devices will all be important control measures. We shall suppose that detectors with $13\ \mu\text{m}$ pixels (0.25 arcsec) are used. These should be manufacturable with deep wells - already full well as high as 150,000 electrons has been demonstrated for $8\times 8\ \mu\text{m}$ pixels (Tower, 1999). In the future $13\ \mu\text{m}$ pixels could be optimized for still greater capacity. Anti-blooming capabilities can be incorporated in the detectors, which may reduce the full well capacity. Alternatively, anti-blooming clocking schemes may be used during integrations. To avoid uncontrolled blooming from the brightest stars, (a few really bright ones will be inevitable in a 3° field), a large number of smaller format devices may be preferred. These could be as small as 1024 pixels square, in which case 1300 devices would be needed to tile the 55 cm diameter focal plane. We find below that the read time should be no more than 5 seconds, requiring a realistic 200 kHz pixel rate to read each 1024 square device with a single amplifier.

As a way to minimize the gaps between the individual CCDs we are presently exploring detector packaging techniques which will allow the use of true, 4-side butttable devices using semiconductor industry standard packaging technologies. This development would limit the inter-device gaps to the non-imaging silicon of each detector, which is dominated by clock busses, amplifiers, and, most significantly, I/O bonding pads. With the continued industry-wide trend toward smaller I/O structures, it is not unreasonable to expect $50\mu\text{m}$ bond pads to be sufficient for future CCDs. If we therefore assume uniform gaps of $100\mu\text{m}$ around each CCD, a fill factor of 96% can be obtained.

Cooling requirements are not severe for the CCD mosaic. The criterion is that the dark rate be less than the sky photon rate in the darkest filters. We estimate that even for the U band or the narrowest 3% filter that photon rates will be $> 1.5e^-/\text{pixel}/\text{sec}$. With an MPP device, dark rates less than this can be achieved at a device temperature of about -15 C. It follows also that in the worst case of a 20 second exposure in a dark band a read noise of $\sim 4 e^-$ rms will be acceptable.

While certainly a very large number of devices are required for this project, the CCDs themselves could be manufactured today. The DC shorts yield of several fabrication lines is now over 50%. If 50% of these unshorted thick CCDs are of astronomical quality, a mature lot run will yield about 25% useable devices from 6" silicon wafers at a modern facility. Assuming a 25-50% thinning and packaging yield, the final thinned device yield would be about 5-10% of the starting lot. This would then require about ~ 200 wafers to be fabricated with 100 devices per wafer, after one or two engineering and test lots. Cryogenic DC and AC wafer probing will allow rapid feedback to the fabricator on device quality and yield.

Infrared arrays The main issues for the infrared concern production time and cost for the large number of devices needed. Supposing that HgCdTe with 2048×2048 $15\mu\text{m}$ pixels are used, 250 are needed to fully populate the 3° focal surface. Production of this large a number should be feasible over a period of a few years, but techniques to lower cost need to be developed. For such a large production run, the long wave cut-off could be tailored to suit the application, and would be set at about $2.3\mu\text{m}$. Given that the fill factor already achieved for the HAWAII die is about 88% by area, we project that creative packaging combined with attention to bond pad sizes and locations on the custom multiplexer should allow for a mosaic filling 90% of the focal surface.

3.3. Mechanical considerations

The optical assembly for an 8.4 m primary is short, only 9 meters between the secondary and tertiary, with the primary and camera set midway between. This configuration is advantageous both for making an agile telescope and an inexpensive enclosure. An ideal, alt-azimuth mount would be like that of the LBT (Hill & Salinari, 1998). All three large mirrors would be stiffly mounted between two C rings, supported on a compact azimuth frame that transmits loads directly to a large diameter pier. This concept, developed by Warren Davison, is illustrated in figure 4. The stiffness of the drives gains by the square of the C ring radius, and we find that the large semicircular rings shown, 11 m

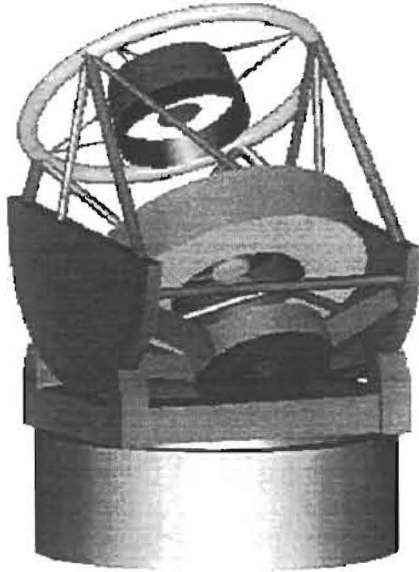


Figure 4. Concept for a rigid, fast-slewing mount. The three mirrors are held between large C rings turning on a flat azimuth platform.

diameter, coupled with the relatively small moment of inertia lead to excellent tracking and stability. Repointing by 3° in a time as short as 5 seconds is realistic. The telescope enclosure will be smaller and hence less expensive than for a standard 8 m telescope, because of the small turning radius.

4. Sensitivity and observing strategies

We have estimated imaging sensitivity in two different ways. First, we have scaled the 10σ point source magnitude limits in the Johnson photometric bands U - H ($0.35 - 1.65 \mu\text{m}$) derived ab-initio by Angel, Dunham, Lesser and Millis (1999) for a 6.5 m telescope. These included the blurring effects of atmospheric seeing and dispersion at 45° elevation. These values are listed in the second column of table 2. Second, limiting magnitudes in the infrared were derived from values computed for an adaptively corrected 8 m ground based telescope by Gillett and Mountain (1998). Corrections have been made for the following differences: 1) Collecting area was scaled for aperture and corrected for 30% vignetting/obscuration loss. 2) Sky aperture to accept 70% source flux was increased to allow for atmospheric seeing, from 0.01 to 0.50 square arcsec. 3) Results were scaled for an integration time of 20 seconds. 4) The Ks band was approximated by halving the bandwidth to $\Delta\lambda/\lambda$ to 0.1. 5) The photon background flux was doubled in Ks band to allow for imperfect telescope baffling.

The 10σ detection limits for unresolved point objects in a 20 second exposure obtained in this way for Johnson magnitudes J, H and Ks are listed in the

third column of table 2. It is encouraging to find good agreement for the J and H bands where the independent calculations overlap.

Table 2. 10σ limits for the 8.4 m telescope.

Band	$\lambda(\text{mm})$	20 second exposure		9 hour exposure
		from Angel et al	from Gillett & Mountain	
U	0.365	22.8	-	26.8
B	0.44	23.8	-	27.8
V	0.55	23.9	-	27.9
R	0.70	23.6	-	27.6
I	0.90	22.8	-	26.8
J	1.25	20.9	20.7	24.8
H	1.65	19.5	19.6	23.5
Ks	2.1	-	18.8	22.8

The depth of these 20 second exposure limits suggested to us one strategy for using the telescope, that of surveying all the observable sky in a sequence of ~ 3000 exposures. Assuming the readout is accomplished while the telescope is repositioned in 5 seconds, 144 exposures an hour could be obtained in clear weather, and the survey would take about 22 hours, i.e. 3-4 nights. In another strategy, a single 3° field could be observed repeatedly during 50 hours of integration time to accumulate deep images in each of the 8 Johnson bands. With sensitivity increased as the square root of the integration time, the 10σ flux limits would be improved by 4 magnitudes to the values given in the last column. The above examples serve as a basis to calculate sensitivities for different strategies that would be used to find variable or moving objects or to obtain better spectral resolution with narrower filters.

5. Comparison with some existing and proposed imaging telescopes

The etendue at the 3° focal plane of our proposed Dark Matter Telescope is $260 (m.^{\circ})^2$, and it will be used with focal plane mosaics with a fill factor of at least 90% for a sampled etendue of $234 (m.^{\circ})^2$. The most powerful imaging telescope currently in operation is the Sloan Digital Sky Survey. It has a modified Cassegrain system with 2.5 m aperture and a 3° field at f/5. Its focal length is 12.5 m, similar to the 8.4 m telescope, and is instrumented with 30 CCDs to sample a field of 1.55 square degrees with 0.4 arcsec pixels, for a sampled etendue of $5.7 (m.^{\circ})^2$. Comparing the 8.4 m telescope with the SDSS, and allowing also for its increased pixel sampling and resolution, the advantage in figure of merit is by a factor of close to 100. The wide field optical cameras to be used with larger telescopes, such as Subaru's Suprime and MMT's Megacam have etendues which are not substantially larger than the SDSS, in the range 5 - 10 $(m.^{\circ})^2$. The recently funded British VISTA telescope is presently conceived as having a 4 m aperture with sampled etendues of 28 $(m.^{\circ})^2$ at optical and 3.1 $(m.^{\circ})^2$ at infrared wavelengths.

At infrared wavelengths, the projected point source sensitivities for the 20 second exposure of table 2 are about 4 magnitudes fainter in J and H than is

being achieved by 2MASS (Cutri, 1999), and about 3.5 magnitudes at Ks. This improvement is consistent with 40 times larger collecting area, 10 times sharper resolution (by solid angle) and 2.5 times longer integration time.

6. Spectroscopy with multiple integral field units

While the main function of the telescope will be imaging, it could be a valuable tool for spectroscopy. It has unique potential for spectroscopic follow up of rare objects with a density of a few to a few hundred in the 3° field. A good example might be the few dozen supernovae with $z \geq 1.5$ found in one field. Because of their small field, standard 8 m telescopes could obtain spectroscopic redshifts of only one or two at a time.

The spectroscopic addition discussed by Angel et al, (1999) used small, individual units to reimage objects on the fibers at longer focal ratio. These units incorporated small prisms, individually motorized for atmospheric dispersion correction. Additional mechanisms corrected continuously for atmospheric anamorphic distortion of the rotating field. The system is thus somewhat complex, and there remain concerns that sky subtraction and coupling efficiency would prevent spectroscopy of the faintest sources.

An attractive alternative is to use multiple, small-scale integral field units. For example, individual fields of 2×3 arcsec could be re-imaged onto 6×9 lenslet arrays subtending $1/3$ arcsec each, that would in turn form pupil images on an array of 54 fiber ends. In this case no mechanisms are needed to correct for either atmospheric dispersion or variable anamorphic distortion with field rotation. Images free from chromatic aberration would be reconstructed from the time sequence of dispersed spectra. The coupling losses in such systems can be kept low, and accurate sky subtraction obtained at the level needed to study the faintest galaxies. If the lenslets were sized at 1 mm, each coupler footprint need be little larger than the 6×9 mm needed for lenslet array, and several hundred units could be placed at once before crowding in the 2000 cm^2 field would become problematic.

Acknowledgments. We are grateful to Bob Millis, Peter Stritmatter, Sidney Wolff for their encouragement and interest in this concept. Reconsideration of the Paul design was stimulated by the recent Lowell workshop on Kuiper belt objects.

References

- Angel, J. R. P., Dunham, T., Lesser, M. & Millis, R. 1999, preprint
Armandroff, T., Bernstein, G. M., Larsen, G., Millis, R. L. Pinto, P. A., Tyson, J. A., Wittman, D. M., & Zaritsky, D. F. 1999, preprint
R. Cutri 1999, 2MASS web page
Gillett, F.C. & Mountain, M. 1998, Science with the NGST, E.P. Smith and A. Koratkar eds, ASP Conf. Series 133, 42-51
Hill, J. M. & Salinari, P. 1998, Proc. SPIE, 3352, 23

- Martin, H. M., Allen, R.G., Angel, J. R. P., Burge, J. H., Davison, W. B., DeRigne, S. T., Dettmann, L. R., Ketelsen, D. A., Kittrell, W. C., Miller, S. M., Stritmatter, P.A., and West, S. C. 1998, Advanced Technology Optical/IR Telescopes VI, Proc. SPIE, 3352, 194-204
- McGraw, J. T., Stockman, H. S., Angel, J. R. P., Epps, H. & Williams, J. T. 1982, Proc SPIE, 331, 137
- Paul, M. 1935, Rev d 'Optique, 14, 169
- Smith, B.K., Burge, J.H., & Martin, H.M. 1997, Optical Fabrication and Testing II, Proc. SPIE, 3134
- Tower, J. R. 1999, Proc. Inter. Conf. on Scientific Optical Imaging IV, M. B. Denton, editor, in press
- Vural, K. 1999, private communication
- Willstrop, R.V. 1984, MNRAS 210, 597 609